

Selective One-Step Synthesis of Dimethoxymethane via Methanol or Dimethyl Ether Oxidation on $H_{3+n}V_nMo_{12-n}PO_{40}$ Keggin Structures

Haichao Liu and Enrique Iglesia*

Department of Chemical Engineering, University of California at Berkeley, Berkeley, California 94720

Received: January 31, 2003; In Final Form: July 10, 2003

The one-step selective synthesis of dimethoxymethane (DMM; $CH_3OCH_2OCH_3$) was achieved by oxidation of dimethyl ether (DME) or methanol (CH_3OH) with O_2 at low temperatures (453–513 K) on unsupported and SiO_2 -supported heteropolyacids with Keggin structures [$H_{3+n}PV_nMo_{12-n}O_{40}$ ($n = 0-4$)]. These materials provide redox and Brønsted acid sites required for bifunctional DMM synthesis pathways. Supported structures at submonolayer coverages (0.1–0.28 Keggin units per nm^2) are much more accessible than bulk structures and remove diffusional constraints. Their higher dispersions lead to marked improvements in DMM synthesis rates and selectivities and to lower CO_x yields using either CH_3OH or DME reactants. The presence of H_2O during DME oxidation increases DMM synthesis rates because of a consequent increase in the rate of DME hydrolysis reactions, which form CH_3OH molecules required as intermediates in the DMM synthesis reaction sequence. Pure CH_3OH reactants form DMM at much higher rates than DME reactants. The replacement of some Mo atoms in $H_3PMo_{12}O_{40}$ structures with V increases DMM synthesis rates and selectivities while inhibiting the formation of CO_x . In fact, CO_x was not detected on $H_{3+n}PV_nMo_{12-n}O_{40}$ ($n = 2, 4$; ~ 0.1 KU/ nm^2) even at high CH_3OH conversions ($\sim 50\%$). CH_3OH converts to DMM via primary CH_3OH reactions to form formaldehyde (HCHO) and subsequent secondary reactions of HCHO with CH_3OH in steps requiring both redox and acid sites; CH_3OH also reacts to form DME on acid sites. These pathways are consistent with the effects of changes in residence time and of the partial removal of acidic OH groups from Keggin structures on reaction selectivities. High CH_3OH pressures and conversions favor HCHO– CH_3OH acetalization reactions and DMM synthesis rates and selectivities. Thermal treatments that cause dehydroxylation and loss of Brønsted acid sites without destroying the primary Keggin structures decrease DME formation rates without significant changes in DMM synthesis rates. These findings suggest that acid sites are not involved in the rate-limiting step for DMM synthesis and that much higher DMM selectivities can be achieved by further increases in the ratio of the rates of redox and acid catalysis. This study represents the first report of high DMM selectivity and yields on stable molecular oxide clusters and provides an effective approach to the rational design of oxide materials for the one-step synthesis of dimethoxymethane from either dimethyl ether or methanol.

1. Introduction

Dimethoxymethane (DMM; $CH_3OCH_2OCH_3$) is an important chemical intermediate. It is used as a gasoline additive, as a building block in organic syntheses, and as a precursor in the synthesis of concentrated formaldehyde (HCHO) streams and of polyoxymethylene dimethyl ethers useful as diesel fuel additives. DMM can be formed from HCHO produced via CH_3OH oxidation reactions. In contrast with the many previous studies of CH_3OH oxidation to formaldehyde, the one-stage syntheses of DMM from CH_3OH



or dimethyl ether (DME) have received limited attention and achieved limited success. Current state-of-the-art DMM synthesis processes involve methanol oxidation to formaldehyde on silver or iron molybdate catalysts, followed by subsequent condensation reactions of methanol–formaldehyde mixtures using sulfuric acid or solid acid catalysts.^{1,2} Iwasawa et al.^{3,4} have recently reported that ReO_x -based catalysts with high Re

content (~ 10 wt %) selectively oxidize methanol to DMM with much higher rates and selectivities than V_2O_5/TiO_2 , molybdophosphoric acid, or $MoO_3/MCM-41$,⁵⁻⁷ typically used for CH_3OH oxidation to HCHO. The high cost of ReO_x and its volatility at the required reaction temperatures ($\sim 473-593$ K) present significant hurdles to the application of this first and only example of a single-stage selective synthesis of dimethoxymethane.

Two types of active sites appear to be required for DMM synthesis. Redox sites with active lattice oxygen atoms are involved in the initial formation of HCHO from CH_3OH or DME, whereas acid sites can catalyze desired acetalization reactions of HCHO and CH_3OH , and also $CH_3OH-CH_3OCH_3$ interconversion side reactions. Heteropolyacids are negatively charged oxide clusters with Keggin structures, W, Mo, or V addenda atoms, and P, Si, or B as central atoms.⁸⁻¹⁰ The negative charge is balanced by cations, which renders the materials acidic when protons become the charge-balancing cations. These solids contain both acid and redox functionalities, but typically form secondary crystalline structures with low surface area (< 10 m^2/g); they would represent attractive potential catalysts for DMM synthesis if their surface area and

* To whom all correspondence should be addressed. E-mail: iglesias@chem.berkeley.edu. Tel: (510) 642-9673. Fax: (510) 642-4778.

TABLE 1: DME Oxidation at 513 K on Unsupported and SiO₂-Supported Heteropolyacid Catalysts (80 kPa DME, 18 kPa O₂, 2 kPa N₂, balance He)

catalyst	DME conversion (%) ^a	rate (DME molecules/KU-h) ^a	rate (mol DME/g-metal-h) ^a	selectivity (%) ^a				
				CH ₃ OH	HCHO	MF	DMM	CO _x
H ₃ PMo ₁₂ O ₄₀	2.0 (1.8)	10.1 (9.2)	8.4 (7.6)	9.9	2.8 (3.1)	16.7 (18.5)	46.0 (51.1)	24.5 (27.2)
H ₅ PV ₂ Mo ₁₀ O ₄₀	1.8 (1.6)	4.4 (3.8)	4.2 (3.6)	13.1	14.8 (17.0)	0.3 (0.3)	56.8 (65.4)	14.9 (17.1)
H ₃ PW ₁₂ O ₄₀	0.9	1.3	0.6	86.8	3.7	0	6.9	2.5
H ₃ PMo ₁₂ O ₄₀ /SiO ₂ (9.3 wt %)	2.3 (2.2)	125.3 (117.4)	103.5 (96.9)	6.3	22.0 (23.5)	15.0 (16.0)	44.6 (47.6)	9.4 (10.0)
H ₅ PV ₂ Mo ₁₀ O ₄₀ /SiO ₂ (9.2 wt %)	1.8 (1.7)	47.7 (44.2)	45.5 (42.1)	7.4	33.2 (35.9)	2.6 (2.8)	55.0 (59.4)	1.8 (1.9)

^a Data in parentheses are calculated on a CH₃OH-free basis.

redox properties could be improved significantly without excessive loss of required Brønsted acid sites.

Heteropolyacids containing W as an addenda atom convert CH₃OH to DME via dehydration reactions catalyzed by Brønsted acid sites, without significant contributions from redox pathways leading to HCHO or DMM.¹¹ Mo-containing heteropolyacids with central Si or P atoms catalyze methanol conversion to formaldehyde with minor amounts of DMM side products.^{6,11} Here, we report the discovery of very active H₃-PMo₁₂O₄₀ and H_{3+n}PMo_{12-n}V_nO₄₀ structures supported on SiO₂, which catalyze CH₃OH reactions at low temperatures with very high selectivities to DMM (80–96%, DME-free basis) and high CH₃OH conversions (20–40%, DME-free basis). These materials also catalyze DMM synthesis from DME (3CH₃OCH₃ + O₂ → 2CH₃OCH₂OCH₃ + H₂O) or DME–CH₃OH reactants. DME and DME–CH₃OH reactants can be produced less expensively from synthesis gas (CO/H₂) than chemical grade CH₃OH,^{12–14} which is currently used in the synthesis of intermediate chemicals.

2. Experimental Section

Supported heteropolyacid catalysts were prepared by incipient wetness impregnation of SiO₂ (Cab-O-Sil, 288 m²/g) with methanolic (Merck, 99.98%) solutions of each heteropolyacid {H_{3+x}PV_xMo_{12-x}O₄₀·30H₂O (x = 0, 1, 2, 4), Japan New Metals Co.; H₃PW₁₂O₄₀·6H₂O, Allen Chem.} at 298 K for 5 h. Impregnated samples were then dried in ambient air at 393 K overnight.

Raman spectra were measured using a HoloLab 5000 Raman spectrometer (Kaiser Optical) and a frequency-doubled Nd:YAG laser at a wavelength of 532 nm. The Raman spectrometer was equipped with a CCD camera that was electrically cooled to 233 K in order to reduce thermal noise. Samples were pressed into self-supporting thin wafers, placed on a rotary stage within a quartz cell, and spun at ~16 Hz to avoid structural changes caused by local laser heating. Raman spectra were measured for fresh samples and for samples treated in flowing 20% O₂/He (O₂, Praxair, 99.999%; He, Airgas, 99.999%; 0.67 cm³/s) at several temperatures for 1 h.

Dimethyl ether and methanol reactions were carried out at 453–533 K in a fixed-bed quartz microreactor containing catalyst powders (0.1–0.3 g) diluted with ground quartz in order to prevent temperature nonuniformities. Samples were treated in flowing 20% O₂/He (O₂, Praxair, 99.999%; He, Airgas, 99.999%; 0.67 cm³/s) for 1.0 h before catalytic reaction measurements. The reactant mixture consisted of 80 kPa DME (Praxair, 99.5%), 18 kPa O₂, and 2 kPa N₂ (Praxair, Certified O₂/N₂ mixture) for DME reactions, and 4 kPa CH₃OH (Merck, 99.98%), 9 kPa O₂, 1 kPa N₂ (Praxair, Certified O₂/N₂ mixture),

and 86 kPa balance He (Airgas, 99.999%) for CH₃OH oxidation reactions. CH₃OH was introduced by bubbling He gas through a glass saturator filled with liquid CH₃OH. For kinetic measurements, CH₃OH and O₂ partial pressures were varied in the range 2–30 kPa, and 5–30 kPa, respectively. Homogeneous DME or CH₃OH reactions were not detected for the conditions used in this study. All transfer lines between the reactor and gas chromatograph were kept above 393 K in order to avoid condensation of reaction products. Reactants and products were analyzed by on-line gas chromatography (Hewlett-Packard 6890GC) using a methyl-silicone capillary (HP-1 with 30 m × 0.25 × 0.25 μm film thickness) column and a Porapak Q packed column (80–100 mesh, 1.82 m × 3.18 mm) connected to flame ionization and thermal conductivity detectors, respectively. Selectivities are reported on a carbon basis as the percentage of the converted reactant appearing as a given product.

3. Results and Discussion

3.1 Catalytic Oxidation of Dimethyl Ether on Heteropolyacids with Keggin Structures. Table 1 shows dimethyl ether (DME) reaction rates and selectivities at 513 K, 80 kPa DME, and 20 kPa O₂ on unsupported and SiO₂-supported H₃PMo₁₂O₄₀ and H₅PV₂Mo₁₀O₄₀ catalysts (treated at 553 K). On both unsupported samples, dimethoxymethane (DMM) was the most abundant reaction product. Reaction rates were normalized per Keggin unit (DME molecules/KU-h) or per gram of V and Mo (mmol/g-metal-h). Reaction rates and selectivities were calculated by considering CH₃OH as a product and as a result, they are reported on a CH₃OH-free basis. At similar DME conversions (~2%), reaction rates were about two times greater on H₃PMo₁₂O₄₀ than on H₅PV₂Mo₁₀O₄₀, but H₅PV₂Mo₁₀O₄₀ was more selective to desired partial oxidation products HCHO (14.8% vs 2.8%) and DMM (56.8% vs.46.0%), and formed less CO_x (CO + CO₂; >90% of CO_x molecules are CO at all reaction conditions) (14.9% vs 24.5%). Methylformate (MF) selectivities were much higher on H₃PMo₁₂O₄₀ (16.7%) than on H₅PV₂Mo₁₀O₄₀ (0.3%). For comparison, the results obtained on H₃-PW₁₂O₄₀ are also included in Table 1. H₃PW₁₂O₄₀ catalysts formed mostly CH₃OH from DME with only traces of HCHO and DMM, consistent with their strong acidity and unreducible nature.^{9,10}

Supporting H₃PMo₁₂O₄₀ (PMo₁₂) and H₅PV₂Mo₁₀O₄₀ (PV₂-Mo₁₀) on SiO₂ led to significantly higher DME oxidation reaction rates, as expected from their greater accessibility compared with their respective crystalline bulk structures (Table 1). At similar surface densities and DME conversions, H₃-PMo₁₂O₄₀/SiO₂ showed higher DME reaction rates than H₅PV₂-Mo₁₀O₄₀/SiO₂, but as in the case of the unsupported samples, H₅PV₂Mo₁₀O₄₀ clusters were more selective for DMM synthesis

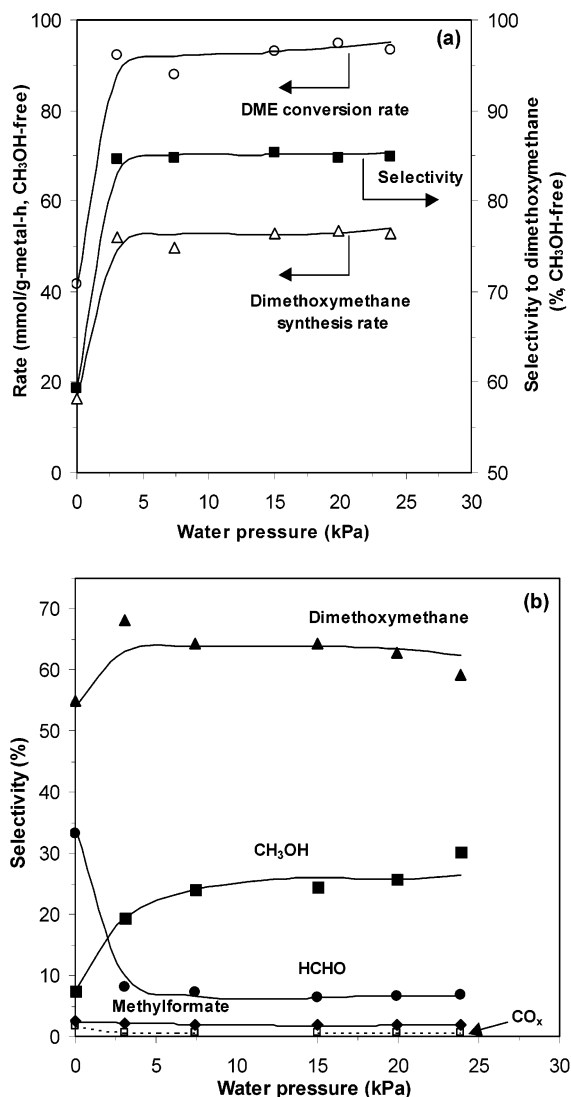


Figure 1. Effects of H₂O partial pressure on oxidative DME reaction rates (CH₃OH-free) (a) and selectivities (b) as well as on CH₃OH-free dimethoxymethane selectivities (a) at 513 K on H₅PV₂Mo₁₀O₄₀/SiO₂ (9.2 wt %) treated at 553 K (80 kPa DME, 18 kPa O₂, 2 kPa N₂, balance He).

than H₃PMo₁₂O₄₀ structures. These supported catalysts showed much lower selectivities to CO_x than the corresponding bulk samples. On both supported catalysts, HCHO selectivities (22 or 33.2%) were higher and DMM selectivities (44.6 or 55.0%) were slightly lower than those in the respective bulk compounds. This may reflect the loss of some Brønsted acid sites during anchoring of Keggin clusters on supports or during subsequent thermal treatments, as also evidenced by the lower CH₃OH selectivities observed on supported samples. On all samples, the relatively high HCHO selectivities appear to reflect the stoichiometric requirement for CH₃OH, which is present in low concentrations, for the final acetalization reaction of HCHO with CH₃OH required in order to form DMM.

Figure 1 shows the effect of adding H₂O to DME reactants during reactions on H₅PV₂Mo₁₀O₄₀/SiO₂ (9.2 wt %; treated at 553 K). These experiments were performed to increase CH₃OH concentrations via acid-catalyzed DME hydration reactions and to allow the completion of the DMM synthesis sequence, which requires an acetalization step and a final step in which CH₃OH reacts with OH groups in adsorbed adducts formed from CH₃OH–HCHO reactants as discussed in detail in the next section. DME conversion rates and DMM synthesis rates

increased by factors of two and three, respectively, and the DMM selectivity increased from 55.0 to 68.3% (59.4 to 84.6%, CH₃OH-free basis) as 3.1 kPa H₂O was added to the DME/O₂ reactant stream. The selectivity to CH₃OH increased concurrently from 7.4 to 19.3% as a result of the higher rate of DME hydration with increasing H₂O concentration (Figure 1b). Higher H₂O concentrations led to additional small increases in DME rates, mostly as a result of slightly higher DME hydration rates and the consequently higher CH₃OH concentrations. The selectivity to DMM increased from 59.4 to 84.6% (CH₃OH-free basis) as the H₂O partial pressure increased to 3.1 kPa, but then remained essentially unchanged (84.7–85.3%) for higher H₂O partial pressures (3.1–23.9 kPa; Figure 1a). Similar H₂O effects were observed on H₃PMo₁₂O₄₀/SiO₂. These general requirements for CH₃OH as a co-reactant in DMM synthesis together with previous literature attempts at direct DMM synthesis from CH₃OH led us to examine this reaction on supported heteropolyacids with Keggin structures.

3.2 Catalytic Oxidation of CH₃OH on Heteropolyacids with Keggin Structures. Effects of H_{3+n}PV_nMo_{12-n}O₄₀ Composition on Oxidative CH₃OH Reactions. The main products formed from CH₃OH reactions on H_{3+n}PV_nMo_{12-n}O₄₀ (*n* = 0,1,2,4) were HCHO, dimethoxymethane, methylformate, and DME (Table 2). At these conditions, CO_x (CO is >90% of the CO_x formed) selectivities were very low (<5%) even at CH₃OH conversions of nearly 70%. Table 2 shows CH₃OH conversion rates (DME-free) and selectivities obtained at 493 K on unsupported and SiO₂-supported H_{3+n}PV_nMo_{12-n}O₄₀ (*n* = 0,1,2,4) catalysts. These materials were treated in dry air at 553 K; the effects of thermal pretreatment temperature are described below. Reaction rates are reported normalized per Keggin unit (molecules/KU-h) and per gram of the active element (mmol/g-metal-h). Selectivities are reported both by considering DME as a products and also on a DME-free basis, in view of available pathways for DME conversion to similar products and to CH₃OH on these catalysts. At similar CH₃OH conversions, reaction rates on the three unsupported heteropolyacids were only weakly influenced by the V/Mo content. DMM was the predominant product of oxidative CH₃OH reactions on all three catalysts and DMM selectivities reached values of 75–81% (DME-free basis at 22–25% CH₃OH conversion).

The replacement of some Mo atoms by V to form H₄PVMo₁₁O₄₀ and H₅PV₂Mo₁₀O₄₀ led to higher DMM selectivities and to lower MF selectivities, as shown in Table 2. The combined selectivity to desired DMM and HCHO products reached values as high as 95% at CH₃OH conversions of 22% (both DME-free basis). High DME selectivities (~50%) were also observed on all crystalline bulk heteropolyacid samples. Unsupported and supported H₃PW₁₂O₄₀ were also tested for CH₃OH–O₂ reactions and they led to the exclusive formation of DME from CH₃OH, consistent with their predominant function as acid catalysts (Table 2).

These materials were also tested as supported samples in order to increase their accessibility to reactants and CH₃OH reaction rates. The results are shown in Table 2. CH₃OH conversion rates increased by a factor of ~40 (both per Keggin unit and per mass of active component). H₄PVMo₁₁O₄₀ clusters supported on SiO₂ were slightly more active than supported H₃PMo₁₂O₄₀, H₅PV₂Mo₁₀O₄₀, and H₆PV₄Mo₈O₄₀ clusters. The selectivity to DME was lower on supported catalysts than on unsupported catalysts, possibly as a result of the loss of some acid sites during anchoring of the Keggin clusters via reaction of their OH groups with Si–OH groups on SiO₂ surfaces. DMM selectivities of ~84% were reached on both H₅PV₂Mo₁₀O₄₀/SiO₂ and H₄-

TABLE 2: CH₃OH Oxidation on Unsupported and SiO₂-Supported Heteropoly Acid Catalysts at 493 K^a and on Other Literature Catalysts for Comparison

catalyst	conversion (%) ^b	rate (DME-free) (molecules/KU-h)	rate (mmol/g-metal-h)	selectivity (%) ^b					refs
				DME	HCHO	MF	DMM	CO _x	
H ₃ PMo ₁₂ O ₄₀	52.6 (24.6)	6.2	5.1 ^c	52.2	4.2 (8.8)	4.2 (9.3)	34.6 (72.3)	5.0 (10.4)	this work
H ₄ PVMo ₁₁ O ₄₀	44.2 (21.2)	5.3	4.8 ^c	52.1	6.5 (13.6)	0.7 (1.4)	38.8 (81.1)	1.7 (3.5)	this work
H ₅ PV ₂ Mo ₁₀ O ₄₀	41.6 (22.4)	5.5	5.2 ^c	48.1	8.7 (16.8)	0.4 (0.8)	40.2 (77.5)	2.6 (5.0)	this work
H ₃ PW ₁₂ O ₄₀	43.2 (trace)	—	— ^c	100	0	0	trace	trace	this work
H ₃ PMo ₁₂ O ₄₀ /SiO ₂ (9.3 wt %)	68.5 (45.7)	248.7	205.7 ^c	33.3	7.6 (11.4)	11.9 (17.9)	41.0 (61.5)	5.5 (8.3)	this work
H ₄ PVMo ₁₁ O ₄₀ /SiO ₂ (9.2 wt %)	68.2 (47.0)	254.2	232.0 ^c	31.1	3.2 (4.6)	5.6 (8.1)	58.1 (84.3)	1.0 (1.5)	this work
H ₅ PV ₂ Mo ₁₀ O ₄₀ /SiO ₂ (9.2 wt %)	63.3 (40.9)	217.4	206.8 ^c	35.4	4.5 (6.9)	4.0 (6.2)	54.0 (83.6)	0.3 (0.4)	this work
H ₆ PV ₄ Mo ₈ O ₄₀ /SiO ₂ (10.2%)	60.3 (41.8)	143.9	154.2	30.7	10.7 (15.4)	2.4 (3.5)	55.1 (79.5)	0	this work
H ₃ PW ₁₂ O ₄₀ /SiO ₂ (9.7%)	92.8 (~0.2)	—	— ^c	99.8	0	0	~0.1 (61.5)	~0.1 (38.5)	this work
SbRe ₂ O ₆ ^d	6.5	—	~1.1	6.5	0	1.2	92.5	0	3
ReO _x /Fe ₂ O ₃ ^e (10 wt Re%)	48.4	—	319.2	1.0	2.4	4.6	91.0	1.0	4
PMo/SiO ₂ ^f (5.75 wt Mo%)	—	—	—	~7	~16	~20	~55	~2	6

^a Reactant mixture: 4 kPa CH₃OH, 9 kPa O₂, 1 kPa N₂, balance He. ^b Data in parentheses are calculated on a DME-free basis. ^c Data are calculated on a DME-free basis. ^d Reaction mixture: CH₃OH/O₂/He = 4.0/9.7/86.3 (mol %); reaction temperature: 573 K. ^e Reaction mixture: CH₃OH/O₂/He = 4.0/9.7/86.3 (mol %); reaction temperature: 513 K. ^f Reaction mixture: CH₃OH/O₂/He = 4.5/10.3/85.2 (mol %); reaction temperature: 513 K; catalysts treated at 593 K.

PVMo₁₁O₄₀/SiO₂ samples at CH₃OH conversions of 40.9–47.0%, with extremely low CO_x selectivities (0.4–1.5%).

Comparison with State-of-the-Art Catalysts for One-Step DMM Synthesis from CH₃OH. The best reported catalysts for direct CH₃OH oxidation to DMM are based on supported Re oxides.⁴ CH₃OH reaction rates (per gram active component, DME-free basis) measured on H₄PVMo₁₁O₄₀/SiO₂ and H₅PV₂Mo₁₀O₄₀/SiO₂ catalysts are similar to the highest values reported on supported ReO_x catalysts (Table 2). DMM selectivities were also similar when compared on a DME-free basis, but the large number of acid sites and strong acidity of heteropolyacid materials led to higher DME selectivities during CH₃OH reactions. Our evaluation of some of the ReO_x-based compositions reported in CH₃OH reactions led to significantly higher DME selectivities than previously reported.⁴ It also led to the extensive sublimation of ReO_x species, consistent with the high volatility of the prevalent ReO_x species at the required reaction conditions. Several other studies have detected DMM products either with very low selectivity or very low formation rate.^{5–7,11} For example, H₃PMo₁₂O₄₀ clusters supported on SiO₂ (5.75 wt % Mo) gave DMM selectivities as high as 55% at 513 K after the sample was treated at 593 K (Table 2), but CH₃OH conversion rates were not reported, thus preventing direct comparisons with our results reported here.⁶ Mo/MCM-41 (2 mol % Mo) showed a high DMM selectivity (72.6%) and very low CH₃OH conversion (0.7%) at 543 K, but Mo migration out of MCM channels led to rapid deactivation.⁷

The partial conversion of CH₃OH to DME during DMM synthesis does not present significant hurdles, because pathways are available for the re-formation of CH₃OH as it is depleted and for DME conversion to HCHO and DMM products on heteropolyacids (Tables 1, Figure 1) and to HCHO on supported MoO_x and VO_x catalysts.^{15–18} Finally, the selectivity to DME can be further decreased by the selective titration of some of the Brønsted acid sites in heteropolyacids or by their partial

dehydroxylation during controlled thermal treatments, as described in the next section.

Effects of H₅PV₂Mo₁₀O₄₀ Surface Density and Thermal Treatment on CH₃OH Reaction Rate and Selectivity. The catalytic properties of supported heteropolyacids depend on their dispersion on SiO₂. Table 3 shows the effects of H₅PV₂Mo₁₀O₄₀ loading and surface density on the rate and selectivity of CH₃OH oxidation reactions. Surface densities are reported as the number of Keggin units or the number of V and Mo active metal atoms per BET surface area (KU/nm² and metal/nm²). For loadings less than 9.2 wt %, reaction rates remained nearly constant with loading, indicating that most, and possibly all, Keggin clusters are accessible to reactants in this surface coverage range. Higher surface densities led to a decrease in CH₃OH reaction rates (per KU), apparently because of incipient agglomeration of dispersed Keggin units into clusters with secondary crystalline structures. The surface densities required for incipient agglomeration (0.10–0.28 KU/nm²) are smaller than those estimated from geometric arguments for a theoretical monolayer of Keggin clusters (0.7 KU/nm²), each one of which occupies ~1.44 nm². The samples with the lowest surface density (0.024 KU/nm²) gave very low DME selectivity (20.4%) and high HCHO selectivity. Increasing the surface density to 0.10 KU/nm² led to higher DME and DMM selectivities and lower HCHO selectivities. At surface densities of 0.65 KU/nm², DMM selectivities decreased and HCHO selectivities increased. It appears that protons are consumed in condensation reactions leading to the anchoring of Keggin clusters at low H₅PV₂Mo₁₀O₄₀ surface densities and that the Keggin clusters may behave similarly to bulk H₅V₂Mo₁₀O₄₀ crystallites as surface densities increase beyond monolayer coverages.

Keggin clusters dehydroxylate via condensation reactions that convert OH groups into H₂O and form Mo–O–Mo linkages between Keggin units and ultimately destroy the primary Keggin structure to form crystalline MoO₃. These reactions occur

TABLE 3: Effects of $\text{H}_5\text{PV}_2\text{Mo}_{10}\text{O}_{40}\cdot 30\text{H}_2\text{O}$ Content of $\text{H}_5\text{PV}_2\text{Mo}_{10}\text{O}_{40}/\text{SiO}_2$ on CH_3OH Oxidation (493 K, 4 kPa DME, 9 kPa O_2 , 1 kPa N_2 , Balance He)

content (wt %)	SA (m^2/g)	SD (KU/nm^2)	SD Mo+V/ nm^2	conversion (%) ^a	rate (DME-free) (molecules/ $\text{KU}\cdot\text{h}$)	rate (DME-free) ($\text{mmol}/\text{g}\cdot\text{metal}\cdot\text{h}$)	selectivity (%) ^a				
							DME	HCHO	MF	DMM	CO_x
2.5	271.1	0.024	0.3	27.2 (21.6)	210.8	201.8	20.4	21.4 (26.9)	4.6 (5.8)	52.7 (66.3)	0
5.1	263.3	0.051	0.6	33.7 (22.0)	210.8	201.0	34.7	14.9 (22.8)	4.2 (6.4)	45.8 (70.1)	0
9.2	236.2	0.10	1.2	44.5 (28.9)	230.7	219.2	35.0	7.2 (11.1)	3.1 (4.8)	53.0 (81.6)	0.1 (0.2)
20.1	190.5	0.28	3.3	41.3 (26.2)	190.9	181.9	36.5	8.1 (12.8)	2.7 (4.3)	51.2 (80.6)	0
35.0	143.1	0.65	7.8	36.9 (23.9)	150.0	142.7	35.2	16.8 (25.9)	2.9 (4.5)	43.4 (67.0)	1.1 (1.6)

^a Data in parentheses are calculated on a DME-free basis.

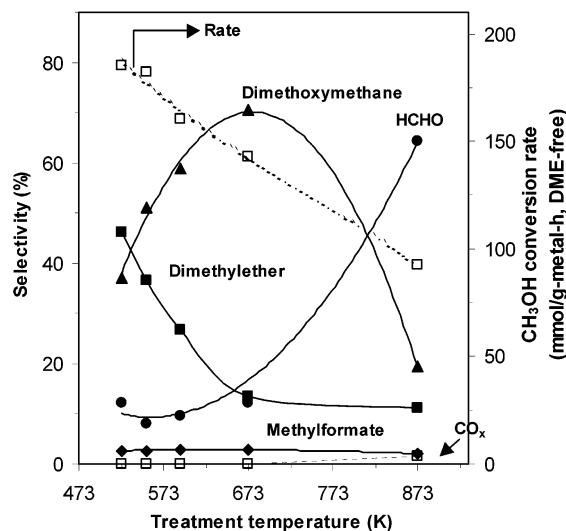


Figure 2. Effects of treatment temperature on CH_3OH conversion rates (DME-free) and selectivities at 493 K on $\text{H}_5\text{PV}_2\text{Mo}_{10}\text{O}_{40}/\text{SiO}_2$ (20.1 wt %; 4 kPa CH_3OH , 9 kPa O_2 , 1 kPa N_2 , balance He).

between 550 and 670 K for bulk $\text{H}_5\text{PMo}_{12}\text{O}_{40}$. The effects of thermal pretreatment on CH_3OH reaction rate and selectivity on supported $\text{H}_5\text{V}_2\text{Mo}_{10}\text{O}_{40}$ were explored and the results are shown in Figure 2. Thermal treatments of $\text{H}_5\text{PV}_2\text{Mo}_{10}\text{O}_{40}/\text{SiO}_2$ (20.1 wt %) in air at 523 K led to high DME selectivities (46.2%) and to relatively low DMM selectivities of 37.1% (69.0%, DME-free). As the thermal treatment temperature increased to 553 K, the DME selectivity declined to 36.5%, while the DMM selectivity increased to 51.2% (80.6%, DME-free). This trend continued until the treatment temperatures reached ~ 673 K. After treatment at 673 K, the DME selectivity was 13.4%, and the DMM selectivity was 70.5% (81.4%, DME-free). Further increases in the thermal treatment temperature (873 K) led to a sharp decrease in DMM selectivity and to a concurrent increase in HCHO selectivity. The reaction rates (DME-free) decreased from 185.4 $\text{mmol}/\text{g}\cdot\text{metal}\cdot\text{h}$ to 143.0 $\text{mmol}/\text{g}\cdot\text{metal}\cdot\text{h}$ by only $\sim 20\%$ as the treatment temperature increased from 553 to 673 K, but then decreased sharply to 92.4 $\text{mmol}/\text{g}\cdot\text{metal}\cdot\text{h}$ after treatment at 873 K (Figure 2).

These changes in the catalytic behavior of $\text{H}_5\text{PV}_2\text{Mo}_{10}\text{O}_{40}/\text{SiO}_2$ (9.2 wt %) upon thermal treatment are consistent with the observed structural evolution of $\text{H}_5\text{PV}_2\text{Mo}_{10}\text{O}_{40}$ Keggin units on SiO_2 surfaces. Figure 3 shows Raman spectra for $\text{H}_5\text{PV}_2\text{Mo}_{10}\text{O}_{40}/\text{SiO}_2$ (9.2 wt %) after exposure to ambient air at 298 K and after treatment in dry air at various temperatures. The samples initially showed Raman bands at 1002 (s), 984 (sh), and ~ 900 (w) cm^{-1} in the 600–1100 cm^{-1} spectral region. The bands at 1002 and 984 cm^{-1} are assigned to terminal Mo=O

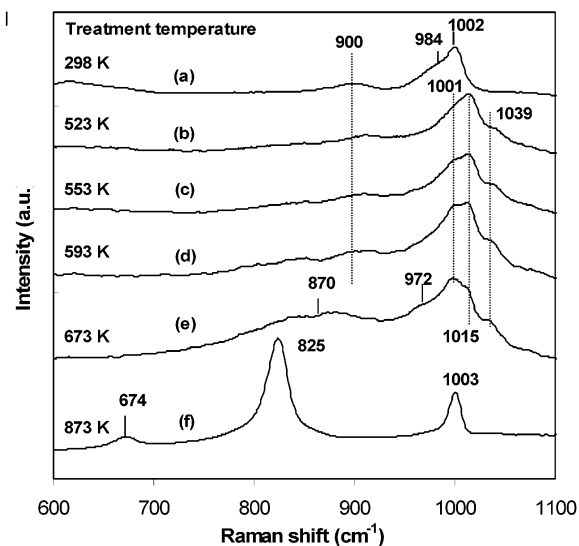


Figure 3. Raman spectra for $\text{H}_5\text{PV}_2\text{Mo}_{10}\text{O}_{40}/\text{SiO}_2$ (20.1 wt %) at 298 K (a) and after thermal treatment in 20% O_2/He at 523 K (b), 553 K (c), 593 K (d), 673 K (e), and 873 K (f).

stretching vibrations, and the band around 900 cm^{-1} is assigned to bridging Mo–O–Mo (or P) stretching modes in the intact Keggin structure.¹⁹ The terminal Mo=O stretching bands at 1002 and 984 cm^{-1} shifted to higher frequencies (1015 and 1001 cm^{-1} , respectively) after treatment in 20% O_2/He at 523 K; the band at ~ 900 cm^{-1} remained unchanged, and a new weak band appeared at 1039 cm^{-1} (Figure 3, curve b). The observed shift to higher frequencies upon water desorption reflects a change in Mo coordination and in the bond order for terminal Mo=O bonds associated with desorption of water molecules loosely coordinated to Keggin structure,¹⁹ as also found for dispersed MoO_x catalysts.^{18,20} The new band detected at 1039 cm^{-1} has been tentatively assigned to vanadyl species, which appear to form via expulsion of some V-atoms from the Keggin structure after treatment at ~ 523 K.¹⁹ Increasing the treatment temperature from 523 to 553 K led to stronger features at 1001 cm^{-1} relative to those at 1015 cm^{-1} , and this trend continued up to 673 K. This phenomenon appears to reflect the loss of protons via dehydroxylation and the consequent formation of condensed Keggin structures after thermal treatment at 523–673 K. Treatment at 673 K led to two additional bands at 972 (w) and ~ 870 cm^{-1} (b). After exposure to ambient moisture, the original spectrum in the starting material was restored (Figure 3, curve a), indicating that dehydroxylation processes are reversible at these temperatures and that destruction of the Keggin structure and formation of crystalline MoO_3 does not occur upon dehydroxylation at 673 K or lower temperatures in these

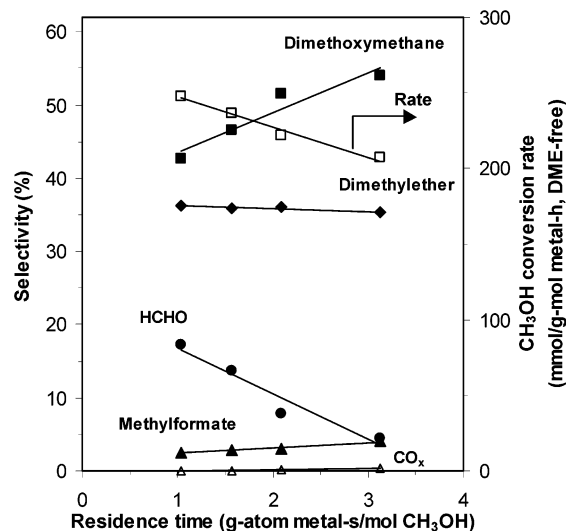


Figure 4. CH_3OH reaction rates (DME-free) and selectivities as a function of reactant residence time at 493 K on $\text{H}_5\text{PV}_2\text{Mo}_{10}\text{O}_{40}/\text{SiO}_2$ (9.2 wt %) treated at 553 K (4 kPa CH_3OH , 9 kPa O_2 , 1 kPa N_2 , balance He).

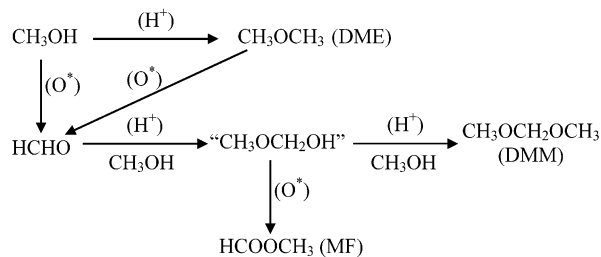
samples. Thermal treatments at 873 K led to the destruction of the Keggin structure in $\text{H}_5\text{PV}_2\text{Mo}_{10}\text{O}_{40}$ and to the irreversible formation of MoO_3 crystallites (Figure 3, curve f), as shown by the characteristic Raman bands at 674, 825, and 1003 cm^{-1} ,²⁰ which remain after exposure to ambient moisture.

The dehydroxylated Keggin structures of $\text{H}_5\text{PV}_2\text{Mo}_{10}\text{O}_{40}$ formed after treatment at $\sim 673\text{ K}$ appear to provide an effective compromise between the redox sites required to form HCHO intermediates and the acid sites involved in acetalization $\text{HCHO}-\text{CH}_3\text{OH}$ reactions to form DMM and in CH_3OH dehydration to form DME. The ultimate decomposition of $\text{H}_5\text{PV}_2\text{Mo}_{10}\text{O}_{40}$ into crystalline MoO_3 and V_2O_5 removes all Brønsted acidity as all OH groups are removed as H_2O , but the materials retain some of the redox properties typical of Mo and V oxides and form HCHO with high selectivity, as in the case of MoO_x - and VO_x -based CH_3OH oxidation catalysts.

Dimethoxymethane Synthesis Pathways and Effects of Reactant Residence Time on Reaction Rates and Selectivities. Figure 4 shows CH_3OH conversion rates and selectivities as a function of reactant residence time, which was changed by varying the reactant space velocity at 493 K on a $\text{H}_5\text{PV}_2\text{Mo}_{10}\text{O}_{40}/\text{SiO}_2$ (9.2 wt %) sample treated at 553 K. The observed trends are similar on all supported and unsupported samples examined in this study.

CH_3OH conversion rates decreased slightly with increasing residence time. This decrease reflects weak kinetic inhibition by water formed during oxidation reactions, as reported previously for DME oxidation to HCHO on MoO_x and VO_x catalysts.¹⁷ The selectivity to the predominant DMM product increased with increasing residence time and CH_3OH conversion, while HCHO selectivity concurrently decreased. Selectivity to MF also increased with increasing residence time. The selectivity to CO_x was always very low ($<0.3\%$) and often undetectable. DME selectivities were essentially independent of residence time. The concurrent increase in DMM and MF selectivities and decrease in HCHO selectivity as residence time increases indicates that DMM and MF form via secondary HCHO reactions. The weak residence time effects on DME selectivity reflect its lower reactivity in oxidation reactions compared with CH_3OH , which is also present at much higher concentrations than DME at these conditions (cf. Tables 1 and 2). The observed effects of residence time on selectivity are

SCHEME 1: Proposed CH_3OH Reaction Pathways.



consistent with the reaction pathways shown in Scheme 1. These pathways include primary CH_3OH reactions to form DME and HCHO, and secondary reactions of HCHO to form DMM and MF via methoxymethanol or hemiacetal ($\text{CH}_3\text{OCH}_2\text{OH}$) intermediates, which form via acetalization reactions of HCHO with methoxide or methanol.^{21,22} $\text{CH}_3\text{OCH}_2\text{OH}$ intermediates were not detected during CH_3OH reactions because of their thermodynamic instability and their expected rapid reactions with CH_3OH to form DMM. These rapid reactions of HCHO and $\text{CH}_3\text{OCH}_2\text{OH}$ intermediates with CH_3OH make DMM appear to behave as a primary product, giving a nonzero extrapolated selectivity at zero residence time (Figure 4). The low measured CO_x selectivities ($<0.5\%$) allow us to exclude these steps from our kinetic analysis of these reaction pathways. DME oxidation kinetic measurements (Table 1 and Figure 1) suggest that secondary reactions of DME formed in CH_3OH reactions can also form HCHO, which subsequently converts to DMM and MF (Scheme 1). These reaction pathways (Scheme 1) require the involvement of bifunctional pathways requiring both redox and acid sites. Redox sites with active lattice oxygen atoms catalyze initial oxidative dehydrogenation reactions of CH_3OH or DME to form HCHO, while acid sites (H^+) are involved in the formation of $\text{CH}_3\text{OCH}_2\text{OH}$ intermediates and in their conversion to DMM, as well as in CH_3OH dehydration to form DME. These conclusions are consistent with the use of monofunctional acid catalysts for reactions of HCHO and CH_3OH to form DMM²³ and with parallel studies of the effects of titration of Brønsted acid sites with organic bases during CH_3OH oxidation reaction on these materials.²⁴ Methylformate is likely to form via oxidative or non-oxidative dehydrogenation of $\text{CH}_3\text{OCH}_2\text{OH}$ intermediates on redox sites. These findings and conclusions indicate that high HCHO concentrations, favored at high CH_3OH conversions or high CH_3OH inlet pressures, lead to higher DMM synthesis rates and selectivities, as a result of faster secondary acetalization reactions involving HCHO and CH_3OH , as shown in the next section.

Reactant Concentration and Temperature Effects on CH_3OH Conversion to Dimethoxymethane. Table 4 shows the effects of reaction temperature on CH_3OH conversion rates and selectivities on $\text{H}_5\text{PV}_2\text{Mo}_{10}\text{O}_{40}/\text{SiO}_2$ (9.2 wt %) samples treated at 553 K. Rates and selectivities are compared at similar CH_3OH conversion levels ($\sim 27\%$, DME-free), which were achieved by varying reactant space velocities over a broad range. CH_3OH reaction rates increased from 68 mmol/g-metal-h to 340 mmol/g-metal-h as reaction temperatures increased from 453 to 513 K. DMM selectivities decreased from 91.8% (DME-free) to 51.1% in this temperature range, mostly as a result of a concurrent increase in HCHO selectivity with increasing reaction temperature. These effects suggest that redox reactions leading to HCHO increase more strongly with temperature than acetalization reactions leading to DMM, suggesting a higher activation energy for the former reactions. DME and MF selectivities were only weakly affected by reaction temperature.

TABLE 4: Effects of Reaction Temperature on CH₃OH Oxidation on H₅PV₂Mo₁₀O₄₀/SiO₂ (9.2 wt %, 4 kPa DME, 9 kPa O₂; Catalyst Sample Treated in Dry Air at 553 K)

temperature (K)	conversion (%) ^a	rate (DME-free) (mmol/g-metal-h)	selectivity (%) ^a				
			DME	HCHO	MF	DMM	CO _x
453	39.9 (26.9)	68.0	32.7	2.1 (3.1)	3.2 (4.8)	61.8 (91.8)	0
473	39.3 (26.1)	132.0	33.6	4.2 (6.3)	3.3 (5.0)	57.9 (87.2)	0
493	45.2 (28.9)	219.2	35.0	7.2 (11.1)	3.1 (4.8)	53.0 (81.6)	0.1 (0.2)
513	42.4 (27.3)	340.4	36.0	24.6 (38.4)	3.8 (6.0)	32.7 (51.1)	0.5 (1.9)

^a Data in parentheses are calculated on a DME-free basis.

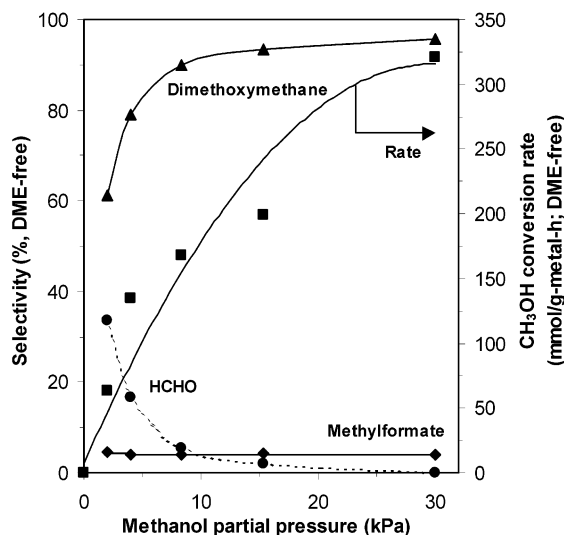


Figure 5. Effects of CH₃OH partial pressure on CH₃OH conversion rates and selectivities on a DME-free basis at 473 K on H₅PV₂Mo₁₀O₄₀/SiO₂ treated at 553 K (9.2 wt %; 9 kPa O₂, 1 kPa N₂, balance He).

Figure 5 shows the effects of CH₃OH partial pressure on CH₃OH conversion rates and selectivities at 473 K on H₅PV₂Mo₁₀O₄₀/SiO₂ (9.2 wt %, treated at 553 K). At similar CH₃OH conversions (~11% DME-free basis), reaction rates increased as CH₃OH partial pressures increased from 2 to 30 kPa. Higher CH₃OH partial pressures led to much lower HCHO selectivities and to a concurrent increase in DMM selectivities from 61.3% to 95.8% (DME-free). These trends appear to reflect the secondary nature of the pathways required for DMM synthesis, which require sequential bimolecular coupling reactions between HCHO and CH₃OH-derived intermediates and between the products formed in this reaction and CH₃OH (Scheme 1). The enhancement of these secondary reactions with increasing CH₃OH partial pressure leads to higher HCHO conversion rates relative to its formation rate and to the observed decrease in HCHO selectivity as CH₃OH inlet pressures increase. The concurrent observed increase in DME selectivity from 32.1% to 51.2% is consistent with the expected bimolecular nature of CH₃OH dehydration reactions.

CH₃OH reaction rates and selectivities were essentially unchanged as O₂ partial pressures increased from 5 to 30 kPa as shown in Figure 6. Such insensitivity to gas-phase O₂ concentrations is typical of catalytic oxidation reactions proceeding via Mars van Krevelen pathways²⁵ using lattice oxygen atoms. Such pathways have been established for CH₃OH²⁶ and DME^{17,18} oxidation to HCHO and for oxidative dehydrogenation of alkanes.^{27,28} The involvement of lattice oxygen atoms in CH₃-

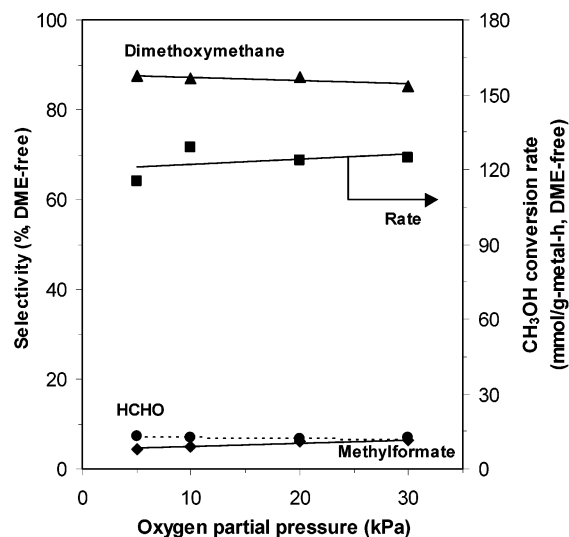


Figure 6. Effect of oxygen pressure on CH₃OH conversion rates and selectivities on a DME-free basis at 473 K on H₅PV₂Mo₁₀O₄₀/SiO₂ treated at 553 K (9.2 wt %; 4 kPa CH₃OH, balance He).

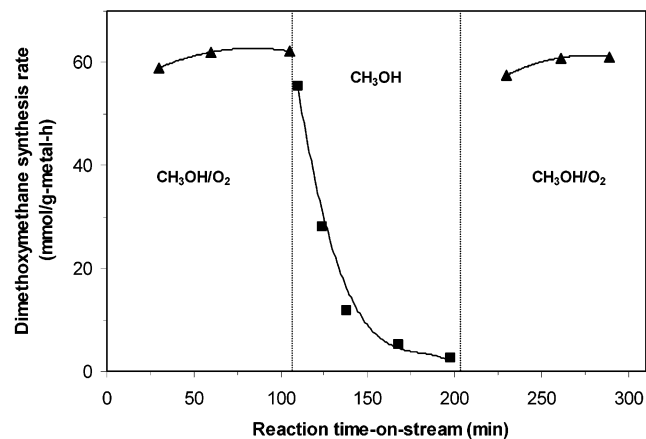


Figure 7. Dimethoxymethane synthesis rates in the presence and in the absence of gas-phase O₂ at 453 K on a steady-state H₅PV₂Mo₁₀O₄₀/SiO₂ catalyst (9.2 wt %) treated at 553 K (4 kPa CH₃OH, 9 kPa O₂ or no O₂, balance He).

OH conversion to DMM was confirmed by transient CH₃OH reaction methods on H₅PV₂Mo₁₀O₄₀/SiO₂ (9.2 wt %, treated at 553 K).

These transient experiments were conducted by carrying out steady-state CH₃OH oxidation reactions on H₅PV₂Mo₁₀O₄₀/SiO₂ catalysts and then removing the gas-phase O₂. Figure 7 shows that the removal of O₂ led to initial rates very similar to those obtained in the presence of O₂ co-reactants, indicating that lattice oxygen is available for CH₃OH conversion reactions. These rates decreased with time as lattice oxygen was depleted by these

CH₃OH oxidation reactions. The reintroduction of O₂ led to the rapid and complete recovery of catalytic CH₃OH conversion rates and selectivities. These findings are consistent with the involvement of lattice oxygen in CH₃OH conversion to DMM and with the rapid reoxidation of the reduced centers formed during the reduction steps in the catalytic sequence, which in turn leads to the weak kinetic consequences of O₂ pressures on DMM synthesis reactions.

4. Conclusions

The one-step selective synthesis of dimethoxymethane via oxidation of dimethyl ether or methanol with O₂ was achieved at low temperatures (453–513 K) on unsupported and SiO₂-supported heteropolyacids with H_{3+n}PV_nMo_{12-n}O₄₀ ($n = 0-4$) stoichiometry and Keggin cluster structures. The required bifunctional pathways benefit from the concurrent presence of redox and Brønsted acids, the ratio of which was varied by controlled thermal dehydroxylation of these Keggin clusters. The anchoring of these clusters on SiO₂ supports increases the accessibility of acid and redox sites and the rate of CH₃OH and CH₃OCH₃ conversion to dimethoxymethane. The replacement of some Mo atoms by V in H_{3+n}PV_nMo_{12-n}O₄₀ increases the rate and selectivity of DMM synthesis from both reactants. CO_x formation is undetectable on several supported H_{3+n}PV_nMo_{12-n}O₄₀ compositions even at high CH₃OH conversion (e.g. ~45%, DME-free). Controlled thermal dehydroxylation leads to partial loss of acid sites and to lower rates and selectivities for CH₃OH dehydration side reactions. These dimethoxymethane selectivities (DME-free basis) and rates on H_{3+n}PV_nMo_{12-n}O₄₀ clusters supported on SiO₂ at 0.1–0.28 KU/nm² surface densities are similar to those reported previously from CH₃OH reactants on ReO_x catalysts. This study also represents the first report of dimethoxymethane synthesis from dimethyl ether. The required bifunctional pathways involve primary reactions of CH₃OH or DME to form HCHO and secondary reaction of HCHO intermediates (formed in redox reactions) with CH₃OH in acetalization and dehydration reactions leading to DMM. High CH₃OH conversions and inlet pressures increase the concentrations of HCHO intermediates and favor secondary reactions and high DMM selectivities and yields.

Acknowledgment. This study was supported by BP as part of the Methane Conversion Cooperative Research Program at the University of California at Berkeley. We acknowledge helpful technical discussions with Drs. Theo Fleisch and John Collins of BP.

Note Added after ASAP Posting. This paper was posted ASAP on 9/10/2003. The middle initial given for Haichao Liu was in error; there is no middle initial. The corrected version was posted 9/16/2003.

References and Notes

- (1) Hagen, G. P.; Spangler, M. J. U.S. Patent 6,265,528, 2001.
- (2) Hagen, G. P.; Spangler, M. J. U.S. Patent 6,437,195, 2002.
- (3) Yuan, Y.; Liu H.; Imoto, H.; Shido, T.; Iwasawa, Y. *J. Catal.* **2000**, *195*, 51.
- (4) Yuan, Y.; Shido, T.; Iwasawa, Y. *J. Phys. Chem. B* **2002**, *106*, 4441.
- (5) Busca, G.; Elmi, A. S.; Forzatti P. *J. Phys. Chem.* **1987**, *91*, 5236.
- (6) Rocchiccioli-Deltchff, C.; Aoussi, A.; Fournier, M. *J. Mol. Catal.* **1996**, *114*, 331.
- (7) Shannon, I. J.; Maschmeyer, T.; Oldroyd, R. D.; Sankar, G.; Thomas, J. M.; Che., M. *J. Chem. Soc., Faraday, Trans.* **1998**, *94*, 1495.
- (8) Pope, M. T. "Heteropoly and Isopoly Oxometalates"; Springer: Berlin, 1983.
- (9) Okuhara T.; Mizuno, N.; Misono, M. *Adv. Catal.* **1994**, *41*, 113.
- (10) Mizuno, N.; Misono, M. *Chem. Rev.* **1994**, *41*, 113.
- (11) Sorensen, C. M.; Weber, R. S. *J. Catal.* **1993**, *142*, 1.
- (12) Li, J.-L.; Zhang, X.-G.; Inui, T. *Appl. Catal., A* **1996**, *147*, 23.
- (13) Fleisch, T. H.; Basu, A.; Gradassi, M. J.; Masin, J. G. *Stud. Surf. Sci. Catal.* **1997**, *107*, 117.
- (14) Shikada, T.; Ohno, Y.; Ogawa, T.; Ono, M.; Mizuguchi, M.; Tomura, K.; Fujimoto, K. *Stud. Surf. Sci. Catal.* **1998**, *119*, 515.
- (15) Liu, H.; Iglesia, E. *J. Catal.* **2002**, *208*, 1.
- (16) Liu, H.; Iglesia, E. U.S. Patent Application, February, 2002.
- (17) Liu, H.; Cheung, P.; Iglesia, E. *J. Phys. Chem. B* **2003**, *107*, 4118.
- (18) Liu, H.; Cheung, P.; Iglesia, E. *J. Catal.* **2003**, *217*, 222.
- (19) Mestl, G.; Ilkenhans, T.; Spielbauer, D.; Dieterle, M.; Timpe, O.; Krohnert, J.; Jentoft, F.; Knozinger, H.; Schlögl, R. *Appl. Catal., A* **2001**, *210*, 13.
- (20) Mestl, G.; Srinivasan, T. K. *Catal. Rev. Sci. Eng.* **1998**, *38*, 451.
- (21) Wachs, I. E.; Madix, R. J. *Surf. Sci.* **1978**, *76*, 531.
- (22) Louis, C.; Tatibouet, J.-M.; Che, M. *J. Catal.* **1988**, *109*, 354.
- (23) Satoh, S.; Tanigawa, Y. U.S. Patent 6,379,507, 2002.
- (24) Liu, H.; Bayat, N.; Iglesia, E. *Angew. Chem. Int. Ed.*, in press.
- (25) Mars, P.; van Krevelen, D. W. *Chem. Eng. Sci.* **1954**, *3*, 41.
- (26) Tatibouet, J. M. *Appl. Catal., A* **1997**, *148*, 213.
- (27) Chen, K.; Iglesia, E.; Bell, A. T. *J. Phys. Chem. B* **2001**, *105*, 646.
- (28) Chen, K.; Bell, A. T.; Iglesia, E. *J. Catal.* **2002**, *209*, 35.